ELSEVIER

Surface Science 490 (2001) L602–L608

SURFACE SCIENCE

www.elsevier.com/locate/susc

Surface Science Letters

Si(1 1 3) hydrogen desorption kinetics: a temperature programmed desorption study

H. Kim, T. Spila, J.E. Greene *

Department of Materials Science, Fredrick Seitz Materials Research Laboratory, University of Illinois, 104 South Goodwin, Urbana, IL 61801, USA

Received 27 December 2000; accepted for publication 23 May 2001

Abstract

Hydrogen desorption kinetics from Si(1 1 3) surfaces were investigated using D_2 temperature programmed desorption (TPD). For this purpose, clean Si(1 1 3)3 × 2 wafers were exposed to atomic deuterium at 200°C for times sufficient to provide D coverages θ_D ranging up to saturation, $\theta_{D,sat}$. Corresponding low-energy electron diffraction patterns transform from 3 × 2 to 3 × 1-D to 1 × 1 with increasing θ_D. TPD spectra from Si(1 1 3) surfaces with $\theta_D = \theta_{D,sat}$ consist of a first-order desorption feature (β_1) centered at 515°C and a second-order desorption peak (β_2) at 405°C. β_2 is assigned to D_2 desorption, with an activation energy of 2.16 eV, from a dideuteride surface phase while β_1 is due to desorption from monodeuteride. The β_1 peak consists of two components: $\beta_{1,t}$ which arises due to first order, as a result of π-bond induced ordering, D_2 desorption from tetramers and $\beta_{1,ad}$ which is due to second-order D_2 desorption from adatoms and second-layer surface atoms. Both β_1 components have activation energies of 2.58 eV. Following monodeuteride desorption, the clean Si(1 1 3) surface again exhibits a 3 × 2 reconstruction. The TPD results are explained based upon previously proposed models for the Si(1 1 3)3 × 2 reconstructed surface. © 2001 Published by Elsevier Science B.V.

Keywords: Silicon; Deuterium; Thermal desorption spectroscopy; Low energy electron diffraction (LEED)

The Si(1 1 3) surface is of interest for both scientific and technological reasons. The surface energy of Si(1 1 3) has been shown to be comparable to that of the low index Si planes (0 0 1), (1 1 1), and (0 1 1) [1]. Thus, 1 1 3 faceting often occurs during Si epitaxy. For example, 1 1 3 facets are observed to form during Si(0 0 1) layer growth in the presence of small amounts of C contamination [2], during Si(0 0 1) lateral epitaxial overgrowth of SiO_2 [3], and during ultra-highly B-doped Si(0 0 1) layer growth by gas-source molecular beam epitaxy (GS-MBE) [4,5].

As shown schematically in Fig. 1a, the bulk-terminated Si(1 1 3) structure consists of alternating 0 0 1- and 1 1 1-like terraces, each one-atom-row wide, along the $[3\,3\,\bar{2}]$ direction. The unreconstructed unit cell contains two surface atoms, one with two dangling bonds, characteristic of 0 0 1-like terraces, and one with a single dangling bond corresponding to 1 1 1-like terraces. It has been known for more than 20 years that the

* Corresponding author. Tel.: +1-217-3331370; fax: +1-217-2442278.

E-mail address: greene@mrlxp2.mrl.uiuc.edu (J.E. Greene).

0039-6028/01/$ - see front matter
PII: S0039-6028(01)01340-1

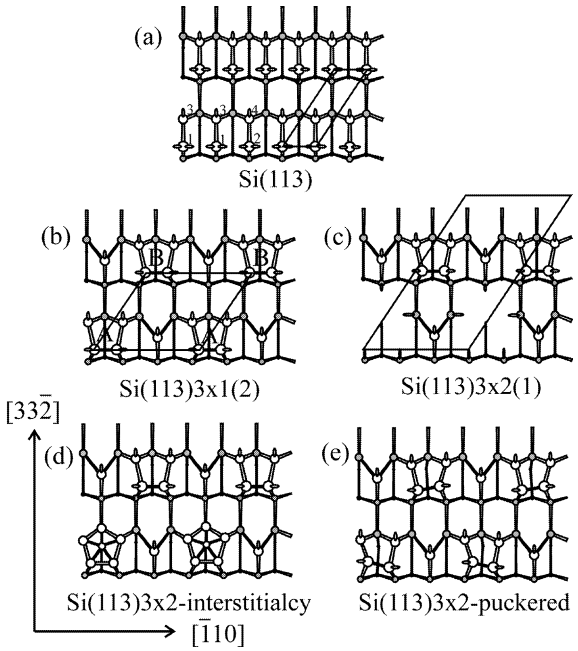

Fig. 1. Surface structure of (a) bulk-terminated Si(1 1 3) and proposed (b) $3 \times 1(2)$, (c) $3 \times 2(1)$, (d) "interstitialcy", and (e) puckering surface reconstruction models. The 1×1, 3×1, and 3×2 unit cells are shown as solid lines.

clean Si(1 1 3) surface exhibits a 3×2 reconstruction [6], but the atom positions in the 3×2 unit cell are still unknown.

The Si(1 1 3) surface structure has been intensely investigated. Early low-energy electron diffraction (LEED) studies indicated that Si(1 1 3) can exhibit either a 3×2 [6] or a 3×1 [7] reconstruction, with the Si(1 1 3)3×2 surface having its threefold and twofold translation vectors along $[\bar{1}\,1\,0]$ and $[3\,3\,\bar{2}]$ directions, respectively. Later, it was shown that sample preparation procedure determines whether 3×2 or 3×1 LEED patterns are observed [8–12]. 3×1 patterns are obtained following annealing at temperatures T_a between 650°C and 800°C, while 3×2 patterns are obtained with $T_a > 800$°C [8–10]. Slow sample cooling rates tend to favor 3×2, independent of T_a [11].

Based upon scanning tunneling microscopy (STM) observations, Knall et al. [14] reported that the Si(1 1 3) surface is composed of small 50–100 Å 3×2 reconstructed domains and suggested that reported 3×1 LEED patterns are due to a decrease in the intensity of the $\times 2$ spots caused by destructive interference among these domains. However, a later STM investigation reported the existence of a distinct 3×1 phase [15]. In addition, several authors have noted that hydrogen adsorption alters the Si(1 1 3) surface reconstruction. [8,11,16–18]. Jacobi et al. [8,9,17,18] found, using LEED and high-resolution electron energy loss spectroscopy (HREELS), that the Si(1 1 3) surface structure changes from 3×2 to 3×1-H to 1×1 with increasing hydrogen exposure at room temperature and that a dihydride phase begins to form when the monohydride peak intensity is nearly saturated. From these observations, they concluded that Si adatoms on the reconstructed Si(1 1 3) surface have only one dangling bond and that the formation of the dihydride phase requires the breaking of Si backbonds [18].

Ranke [13] proposed several possible structural models for the 3×1 and 3×2 reconstructions, two of which are schematically shown in Fig. 1b (the $3 \times 1(2)$ model, following Ranke's notation), and Fig. 1c (the $3 \times 2(1)$ model). Knall et al. reported that the $3 \times 2(1)$ model is consistent with their STM images [14], but Dabrowski et al. [19, 20] suggested a 3×2 "interstitialcy" model (see Fig. 1d) as a modification of Ranke's $3 \times 1(2)$ surface reconstruction and showed that the interstitialcy model has a lower surface energy than $3 \times 2(1)$ while being more consistent with their own STM results. The elementary building blocks for all of these models are the same, a tetramer unit and a 1 1 1-like adatom. More recently, a puckering model was proposed that is also based upon the $3 \times 1(2)$ reconstruction, but with alternate tetramer units buckled in opposite directions [21]. However, there is still no consensus regarding the surface atom positions on either clean reconstructed or H-adsorbed Si(1 1 3).

In this letter, we present the results of an investigation of hydrogen desorption kinetics using D_2 temperature programmed desorption (TPD) and LEED. Quantitative knowledge of hydrogen desorption kinetics is essential for understanding and modeling hydride gas-source film growth on Si(1 1 3) and is also expected to provide additional insight regarding local bonding configurations in

the 3×2 reconstructed surface. Saturation deuterium adsorption on Si(1 1 3) results in a 1×1 LEED structure and yields D_2 TPD spectra with two distinct desorption features, labeled β_2 and β_1. We assign the low-temperature second-order β_2 peak to D_2 desorption, with activation energy $E_a = 2.16$ eV, from a dideuteride surface phase. The high-temperature β_1 monodeuteride feature is composed of two overlapping peaks, $\beta_{1,t}$ and $\beta_{1,ad}$. The $\beta_{1,t}$ peak corresponds to first-order D_2 desorption, due to π-bond-induced ordering, from tetramer units. $\beta_{1,ad}$ arises due to second-order D_2 desorption from adatoms and second-layer surface atoms. Both $\beta_{1,t}$ and $\beta_{1,ad}$ have activation energies $E_a = 2.58$ eV.

All experiments were performed in a multichamber ultra-high-vacuum (UHV) system, described in detail in Ref. [22], with a base pressure of 5×10^{-11} Torr. The analytical chamber is equipped with provisions for GS-MBE layer growth, gas dosing, TPD, reflection high-energy electron diffraction (RHEED), LEED, and Auger electron spectroscopy (AES). D_2 was delivered through a molecular beam doser and a hot W filament in the gas stream was used to crack the gas. For TPD experiments, the sample was placed 2 mm from the 5-mm-diameter hole in the skimmer cone between the mass spectrometer and analytical chambers. Samples were heated at a linear rate, typically $2°C\,s^{-1}$, by direct current while the temperature was determined by a thermocouple calibrated using an optical pyrometer.

The Si(1 1 3) samples used in these experiments were 1×3 cm^2 plates cleaved from 0.5-mm-thick B-doped ($1–2 \times 10^{14}$ cm^{-3}) wafers with a miscut of $\pm 0.25°$ toward [1 1 0]. Initial cleaning consisted of solvent degreasing, multiple wet-chemical oxidation/etch cycles, and a 20 s etch in dilute (10%) HF. The substrates were then exposed to a UV/ozone treatment to remove C-containing species [23] and introduced, through the sample-exchange chamber, into the deposition system where they were degassed at 600°C for 4 h and then heated at $100°C\,s^{-1}$ to 1100°C for 1 min to remove the oxide. After the flash desorption, the substrates were rapidly cooled ($\simeq 20°C\,s^{-1}$) to 900°C then slowly cooled ($\simeq 0.5°C\,s^{-1}$) to 200°C, the temperature at which the D exposures were carried out. Following this procedure, no residual C or O was detected by AES.

Clean Si(1 1 3) samples exhibit 3×2 LEED patterns at temperatures $T_s < 400°C$, 3×1 at $400 < T_s < 700°C$, and 1×1 at $T_s > 700°C$, all in agreement with previous reports [12]. Exposing Si(1 1 3)3×2 surfaces to D at 200°C results first in the formation of a 3×1 surface phase which, with increasing coverage, is gradually converted to 1×1 at saturation D coverage. We note that D-saturated Si(0 0 1)2×1, Si(1 1 1)7×7, and Si-(0 1 1)16×2 surfaces also exhibit 1×1 diffraction patterns [5,24].

Fig. 2 shows typical D_2 TPD spectra from Si(1 1 3)3×2 surfaces exposed to atomic deuterium for times t_D ranging from 6 to 600 s. The data are plotted as a function of D coverage θ_D normalized to saturation coverage $\theta_{D,sat}$ ($t_D \geqslant 600$ s). For D exposures corresponding to $\theta_D/\theta_{D,sat} < 0.54$, the TPD spectra exhibit only one feature, while at higher deuterium coverages an additional lower-temperature peak begins to appear [8,9,17,18]. The position of the high-temperature feature remains constant with $\theta_D/\theta_{D,sat}$ while the low-temperature peak shifts to higher temperatures.

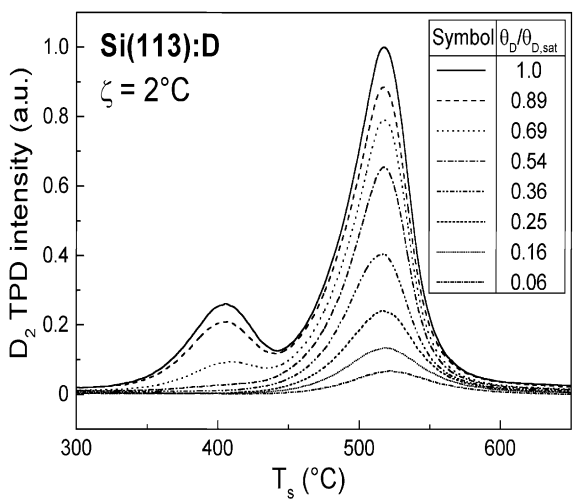

Fig. 2. D_2 TPD spectra, obtained with a heating rate $\zeta = 2°C\,s^{-1}$, from Si(1 1 3) surfaces exposed to atomic deuterium for $t_D = 6$, 15, 30, 60, 120, 180, 300, and 600 s at 200°C.

We fit our TPD spectra using standard Polanyi–Wigner analysis [25] in which the desorption rate $d\theta_D/dT$ is expressed as

$$\frac{d\theta_D}{dT} = -\left(\frac{v}{\zeta}\right)\theta_D^n \exp\left(-\frac{E_a}{kT}\right) \quad (1)$$

where v is the attempt frequency, θ_D is the instantaneous D coverage, E_a is the desorption activation energy, n is the kinetic order of desorption reaction, ζ is the heating rate, and k is Boltzmann's constant. Readsorption can be ignored due to the high pumping speed and the low D_2 sticking probability. For this case [26],

$$\ln\left(\frac{\theta_D(T)}{\theta_0}\right) = -\frac{v}{\zeta}I(T) \quad (2)$$

for first-order desorption and

$$\theta_D(T) = \frac{\theta_0}{1 + (v/\zeta)\theta_0 I(T)} \quad (3)$$

for second-order desorption. θ_0 in Eqs. (2) and (3) is the initial coverage and $I(T)$ is given by

$$I(T) = \frac{E_a}{k}\left|\frac{e^{-\varepsilon}}{\varepsilon^2}\sum_{n=1}^{\infty}\frac{(-1)^{n+1}n!}{\varepsilon^{n-1}}\right|_{T_0}^{T} \quad (4)$$

in which $\varepsilon = E_a/kT$.

Fig. 3a shows a typical Si(1 1 3) TPD spectrum fit with two peaks. Frequency factors and desorption activation energies are 2×10^{15} s^{-1} and 2.58 eV for the high-temperature feature labeled β_1 and 1×10^{15} s^{-1} and 2.16 eV for the low-temperature peak β_2. While β_1 appears to follow first-order desorption kinetics with a peak temperature T_p that remains constant at 515°C, the shape of β_2 indicates second-order kinetics for which T_p decreases from 417°C at $\theta_D/\theta_{D,sat} = 0.54$ to 405°C at saturation coverage. Comparison of Si(0 0 1) D_2 TPD spectra, which also consist of a lower-temperature second-order β_2 peak and a high-temperature first-order β_1 peak [27], with the present Si(1 1 3) results reveals that both the β_1 and β_2 peak shapes and temperatures are very similar in the two sets of spectra. Thus, as for Si(0 0 1), we assign the β_2 Si(1 1 3) TPD peak to D_2 desorption from a dideuteride phase and β_1 to desorption from a monodeuteride phase. The peak fits are everywhere excellent except at the very high temperature (low D coverage, $\theta_D/\theta_{D,sat} < 0.16$) edge of β_1. We will return to this point later.

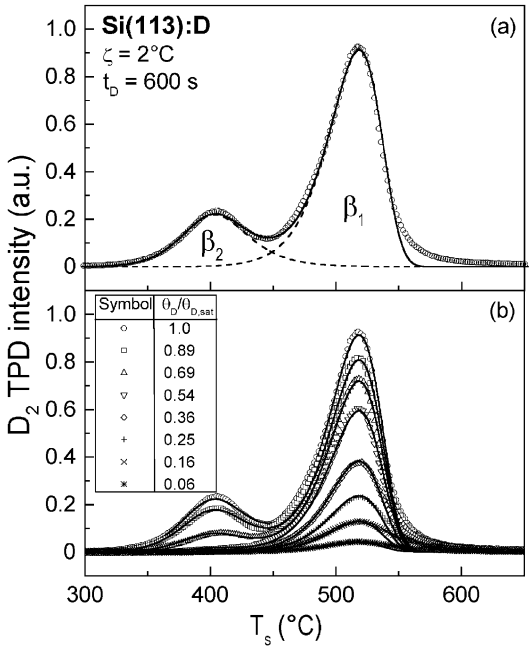

Fig. 3. Fitted D_2 TPD spectra (—) from Si(1 1 3) with (a) saturation deuterium coverage $\theta_{D,sat}$ and (b) $\theta_D/\theta_{D,sat} = 1.0$, 0.89. 0.69, 0.54, 0.36, 0.25, 0.16, and 0.06. β_2 and β_1 arise due to D_2 desorption from dideuteride and monodeuteride phases, respectively.

The primitive unit cell of the unreconstructed Si(1 1 3) surface in Fig. 1a contains two atoms, one with a single dangling bond and one with two dangling bonds. The $3 \times 1(2)$ model (Fig. 1b) is constructed by dimerizing adjacent 0 0 1-like atoms (e.g., the atoms labeled 1 in Fig. 1a) and removing the next 0 0 1-like atom (in this example, atom 2 in Fig. 1a). After atom 2 is removed, atom 4 becomes an adatom as shown in Fig. 1b. The 1,1 dimer, together with its two neighboring 1 1 1-like atoms (labeled 3 in Fig. 1a), form a tetramer unit with $3\times$ periodicity along $[\bar{1}\,1\,0]$ and $\times 1$ alternating-row periodicity along $[3\,3\,\bar{2}]$. Thus, the primitive $3 \times 1(2)$ unit cell in Fig. 1b consists of one tetramer unit and one adatom. This reconstruction decreases the dangling bond (db) density from 1.5 db per surface atom for the unreconstructed surface to 1 db per atom for the $3 \times 2(2)$ surface. The

structure does not, however, explain the $\times 2$ [3 3 $\bar{2}$] periodicity observed in LEED patterns. Thus, the $3 \times 2(1)$ model (Fig. 1c) was introduced in which half of the tetramer units are removed. While this provides the correct surface periodicity and is consistent with some (but not all) reported STM observations of 3×2 domains [14], the $3 \times 2(1)$ to $3 \times 1(2)$ transition requires significant mass transport to create the surface voids. This, however, is inconsistent with the observed reversibility of the $3 \times 2 \leftrightarrow 3 \times 1$ transition [12].

In another attempt to resolve the 3×2 surface structure, Dabrowski et al. [19,20] introduced the "interstitialcy" model in which a Si self-interstitial is located at the centers under tetramers, thus forming pentamer units (Fig. 1d), in alternating rows along [3 3 $\bar{2}$]. Later, Wang et al. [21] proposed the puckering model, in which the 3×2 reconstruction is basically the same as the $3 \times 1(2)$ surface (Fig. 1b) except that adjacent [3 3 $\bar{2}$] tetramer rows are buckled in opposite directions. The alternating puckered structure has a surface energy which is comparable to that of the interstitialcy model and lower than both of Ranke's models by at least 0.12 eV [28]. Recent Kikuchi electron holography images of Si(1 1 3) appear to favor the puckering model [29]. Moreover, 3×1 LEED patterns can be explained within this model by puckering of the tetramer rows in the same direction. Thus, the reversible 3×1 to 3×2 transition is accomplished by simply shifting alternate buckling directions with no mass transport required. However, the puckered Si(1 1 3)3×2 surface contains a mirror glide plane which is not observed in either our or previously reported LEED diffraction patterns.

All the proposed Si(1 1 3)3×2 surface reconstruction models share the same constituent units: a tetramer (or pentamer) and an adatom. Thus, the tetramer unit plays a key role in determining hydrogen desorption kinetics from Si(1 1 3). Based upon STM results, Knall et al. suggested that there is a strong interaction, leading to the formation of π bonds, among the dangling bonds of atoms composing the tetramers [14]. This is analogous to the case for Si(0 0 1)2×1 surfaces, where π-bond-induced ordering of dangling bonds on single dimers gives rise to first-order hydrogen desorption (the Si(0 0 1):H β_1 peak) [30]. Thus, we propose that the first-order β_1 desorption kinetics we observe from Si(1 1 3) is due to π-bond-induced pairing of hydrogen atoms on the tetramer units. The energy gain associated with the π bonds provides the driving force for hydrogen-atom ordering on the tetramer units.

As is the case for adatoms on Si(1 1 1) and Si(0 1 1) surfaces [24] we expect that hydrogen desorption from monohydride adatoms will follow second-order kinetics. However, since there are four dangling bonds on the tetramer unit and only one dangling bond on the adatom, the monodeuteride peak from the tetramer phase $\beta_{1,t}$ dominates and we do not completely resolve the smaller second-order adatom monodeuteride peak $\beta_{1,ad}$. Fig. 4 shows the TPD spectrum in Fig. 3a fit with, in addition to β_2, first-order $\beta_{1,t}$ and second-order $\beta_{1,ad}$ peaks. Both β_1 peaks are centered at $T_p = 515$°C with activation energies $E_a = 2.58$ eV. Equally good fits, including the high temperature (low θ_D) region, were obtained for all samples. In Fig. 4, for which $\theta_D/\theta_{D,sat} = 1$, the integrated TPD peak intensities of the adatom monodeuteride $I_{\beta_{1,ad}}$ and the tetramer monodeuteride $I_{\beta_{1,t}}$ phases are 0.32 and 0.68 ML, respectively, where

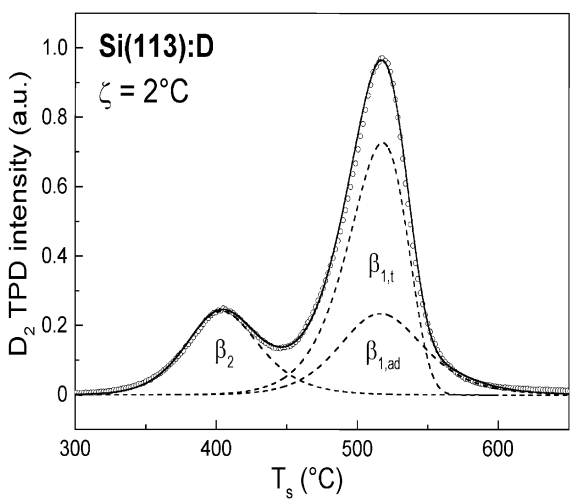

Fig. 4. Fitted D_2 TPD spectra (—) from Si(1 1 3) with saturation deuterium coverage. β_2 results from D_2 desorption from the dideuteride surface phase while $\beta_{1,t}$ and $\beta_{1,ad}$ correspond to D_2 desorption from tetramer and adatom/surface-atom monodeuterides, respectively.

we define 1 ML as the unreconstructed Si(1 1 3) surface atom density, 8.18×10^{14} cm^2. The integrated TPD peak intensity I_{β_2} of the lower-temperature dideuteride phase in Fig. 4 is 0.29 ML.

At D coverages $\theta_D/\theta_{D,sat} < 0.54$, Fig. 2 shows that Si(1 1 3):D TPD spectra contain only the high-temperature β_1 monodeuteride feature. However, at larger deuterium coverages, we observe an additional low-temperature β_2 dideuteride peak which occurs at essentially the same desorption temperature as that of the β_2 dideuteride phase on Si(0 0 1), Si(1 1 1), and Si(0 1 1) [24,27]. Thus, we propose that, as in the case of the low index Si surfaces, deuterium adsorption on Si(1 1 3) at higher coverages results in the breaking of adatom backbonds, which are highly strained, leading to the formation of dideuteride adatoms. This process leaves a second-layer atom with a single dangling bond. At saturation deuterium coverage, therefore, the original surface unit cell contains a monohydride tetramer unit, a first-layer dideuteride adatom, and a second-layer monodeuteride Si atom. During the D_2 TPD experiment, all dideuteride adatoms are converted to monodeuteride adatoms by $\simeq$450–500°C. Thus, the expected $I_{\beta_{1,ad}}$ value should correspond to the ratio of the sum of the contributions from the first-layer adatoms and the second-layer surface atoms. Based upon bond counting, this yields $(1+1)/(1+1+4) = 0.33$ ML, in very good agreement with our measured value of 0.32 ML.

Following a similar argument, the expected I_{β_2} value at $\theta_{D,sat}$ should be $1/6 = 0.167$ ML. However, we obtain 0.29 ML, indicating the formation of additional dideuteride species. The most probable sites are 0 0 1-like dimers in the tetramer units where D atoms can attack the σ-bond, insert, and form two dideuteride species. If this occurred at all tetramer units, I_{β_2} would correspond to $(1+2)/6 = 0.5$ ML. Thus, under the D dosing conditions used here, less than half of the dimers are converted to dideuteride species.

Our TPD results, showing that $I_{\beta_{1,t}} > I_{\beta_{1,ad}}$, allow us to exclude the $3 \times 2(1)$ model for the Si(1 1 3)3×2 reconstruction. In the $3 \times 2(1)$ surface, D saturation would result in more than half of the monodeuteride species residing on adatoms and second-layer surface atom sites. Thus, the Si(1 1 3)$3 \times 2(1)$ surface would have a TPD monodeuteride desorption signature with $I_{\beta_{1,ad}} > I_{\beta_{1,t}}$, the opposite of what we observe. This leaves the puckering and interstitialcy models for which the lack of a mirror glide plane in LEED patterns favors the latter.

In summary, we have determined the kinetic order, frequency factors υ, and activation energies E_a for all three hydrogen desorption paths from Si(1 1 3) surfaces: second-order desorption from dihydride species on adatoms and 0 0 1-like atoms in surface tetramer units, second-order desorption from monohydride species on adatoms and second-layer surface atoms, and first-order desorption from monohydride species on tetramer units. υ and E_a for dihydride and monohydride desorption are 1×10^{15} s^{-1}/2.16 eV and 2×10^{15} s^{-1}/2.58 eV, respectively. The dihydride surface phase is only observed for hydrogen coverages >0.54 ML. We expect, as in the case for Si(0 0 1) [5] and Si(0 1 1) [31] GS-MBE from hydride precursors, that Si(1 1 3) film growth kinetics in the surface-reaction-limited regime will be controlled primarily by the rate of H_2 desorption from the monohydride surface phase. The pathway for this process is first order due to π-bond-induced pairing of hydrogen atoms on surface tetramer units.

Acknowledgements

The authors acknowledge the financial support of the Materials Science Division of the US Department of Energy (DOE) under Award DEF-G02-ER9645439. We also appreciate the use of the Center for Microanalysis of Materials at the University of Illinois, which is supported by the DOE.

References

[1] J.M. Gibson, M.L. McDonald, F.C. Unterwald, Phys. Rev. Lett. 55 (1985) 1765.
[2] Y.-N. Yang, E.D. Williams, J. Vac. Sci. Technol. A 8 (1990) 2481.
[3] H. Hirayama, M. Hiroi, T. Ide, Phys. Rev. B 48 (1993) 17331.
[4] T.R. Bramblett, Ph.D. Thesis, University of Illinois, 1994.

[5] H. Kim, G. Glass, T. Spila, N. Taylor, S.Y. Park, J.R. Abelson, J.E. Greene, J. Appl. Phys. 82 (1997) 2288.
[6] B.Z. Olshanetsky, V.I. Mashanov, Surf. Sci. 111 (1981) 414.
[7] R. Heckingbottom, P.R. Wood, Surf. Sci. 23 (1970) 443.
[8] U. Myler, K. Jacobi, Surf. Sci. 220 (1989) 353.
[9] U. Myler, P. Althaiz, K. Jacobi, Surf. Sci. 251/252 (1991) 607.
[10] Y.-N. Yang, E.D. Williams, R.L. Park, N.C. Bartelt, T.L. Einstein, Phys. Rev. Lett. 64 (1990) 2410.
[11] X. Hu, K. Feng, Z. Lin, Y. Xing, Appl. Surf. Sci. 103 (1996) 101.
[12] Y.R. Xing, J.P. Zhang, J.A. Wu, C.Z. Liu, C.H. Wang, Surf. Sci. Lett. 232 (1990) L215.
[13] W. Ranke, Phys. Rev. B 41 (1990) 5243.
[14] J. Knall, J.B. Pethica, J.D. Todd, J.H. Wilson, Phys. Rev. Lett. 66 (1991) 1733.
[15] M.J. Hadley, S.P. Tear, B. Röttger, H. Neddermeyer, Surf. Sci. 280 (1993) 258.
[16] J.H. Wilson, P.D. Scott, J.B. Pethica, J. Knall, J. Phys. Condens. Matter 3 (1991) S133.
[17] M. Jacobi, U. Myler, Surf. Sci. 284 (1993) 223.
[18] M. Jacobi, M. Gruyters, P. Geng, T. Bitzer, M. Aggour, S. Raucher, H.-J. Lewerentz, Phys. Rev. B 51 (1995) 5437.
[19] J. Dabrowski, H.-J. Müssig, G. Wolff, Phys. Rev. Lett. 73 (1994) 1660.
[20] J. Dabrowski, H.-J. Müssig, G. Wolff, Surf. Sci. 331–333 (1995) 1022.
[21] J. Wang, A.P. Horsfield, D.G. Pettifor, M.C. Payne, Phys. Rev. B 54 (1996) 13744.
[22] N. Taylor, H. Kim, T. Spila, J.A. Eades, G. Glass, P. Desjardins, J.E. Greene, J. Appl. Phys. 85 (1999) 501.
[23] X.-J. Zhang, G. Xue, A. Agarwal, R. Tsu, M.-A. Hasan, J.E. Greene, A. Rockett, J. Vac. Sci. Technol. A 11 (1993) 2553.
[24] H. Kim, N. Taylor, T. Spila, G. Glass, S.Y. Park, J.E. Greene, J.R. Abelson, Surf. Sci. Lett. 380 (1997) L496.
[25] P.A. Redhead, Vacuum 12 (1962) 203.
[26] F.M. Lord, J.S. Kittelberger, Surf. Sci. 43 (1974) 173.
[27] H. Kim, G. Glass, S.Y. Park, T. Spila, N. Taylor, J.R. Abelson, J.E. Greene, Appl. Phys. Lett. 69 (1996) 3869.
[28] D.M. Bird, L.J. Clarke, R.D. King-Smith, M.C. Payne, I. Stich, A.P. Sutton, Phys. Rev. Lett. 69 (1992) 37865.
[29] C.Y. Chang, Y.C. Chou, C.M. Wei, Phys. Rev. B 59 (1999) R10453.
[30] J.J. Boland, J. Vac. Sci. Technol. A 10 (1992) 2458.
[31] N. Taylor, H. Kim, P. Desjardins, Y.L. Foo, J.E. Greene, Appl. Phys. Lett. 76 (2000) 2853.